

RESEARCH

Open Access



# Eco-friendly monitoring of triclosan as an emerging antimicrobial environmental contaminant utilizing electrochemical sensors modified with CNTs nanocomposite transducer layer

Nardine Safwat<sup>1</sup>, Amr M. Mahmoud<sup>2\*</sup>, Maha F. Abdel-Ghany<sup>1</sup> and Miriam F. Ayad<sup>1</sup>

## Abstract

Environmental appearance of antimicrobials due to frequent use of personal care products as recommended by WHO can cause serious flare-up of antimicrobial resistance. In this work, three eco-friendly microfabricated copper solid-state sensors were developed for measuring triclosan in water. Multi-walled carbon nanotubes were incorporated in sensor 2 and 3 as hydrophobic conductive inner layer. Meanwhile,  $\beta$ -cyclodextrin was incorporated in sensor 3 as an ionophore for selective binding of TCS in presence of interfering compounds. The obtained linear responses of sensors 1, 2 and 3 were ( $1 \times 10^{-8}$ – $1 \times 10^{-3}$  M), ( $1 \times 10^{-9}$ – $1 \times 10^{-3}$  M) and ( $1 \times 10^{-10}$ – $1 \times 10^{-3}$  M), respectively. Limit of detection was  $9.87 \times 10^{-9}$  M,  $9.62 \times 10^{-10}$  M, and  $9.94 \times 10^{-11}$  M, respectively. The miniaturized sensors were utilized for monitoring of triclosan in water samples.

**Keywords** Antimicrobial resistance, Coronavirus disease-19, Emerging contaminants, Green analysis, Solid contact ISEs, Triclosan

## Introduction

The outbreak caused by the emergence of COVID-19 disease was announced by the WHO as being pandemic in March 2020. Owing to the absence of vaccines or drugs approved for the treatment of COVID-19 disease to face the global dramatic increase in the infection rates, the WHO has recommended to follow healthy lifestyles and

safety measures in order to prevent the global spread of COVID-19. Excessive use of hand sanitizers, soaps and detergents has raised a great concern to the emergence of antimicrobial resistance which pose a serious threat to public health and global economy. Triclosan; an antimicrobial agent, has been reported as an emerging contaminant in the environment and that issue has escalated and has become disastrous during the pandemic outbreak of COVID-19 [1–3].

The emergence of drug residues, cosmetic products, steroids, surfactants, fragrances, and plasticizers in the environment have been growing in the past decades [4, 5]. These emerging environmental contaminants are any uncommon man-made or natural chemicals or any

\*Correspondence:

Amr M. Mahmoud

amr.bekhet@pharma.cu.edu.eg

<sup>1</sup>Pharmaceutical Analytical Chemistry Department, Faculty of Pharmacy, Ain Shams University, Abbassia 11566, Cairo, Egypt

<sup>2</sup>Pharmaceutical Analytical Chemistry Department, Faculty of Pharmacy, Cairo University, Kasr-El Aini Street, Cairo 11562, Egypt



© The Author(s) 2023. **Open Access** This article is licensed under a Creative Commons Attribution 4.0 International License, which permits use, sharing, adaptation, distribution and reproduction in any medium or format, as long as you give appropriate credit to the original author(s) and the source, provide a link to the Creative Commons licence, and indicate if changes were made. The images or other third party material in this article are included in the article's Creative Commons licence, unless indicated otherwise in a credit line to the material. If material is not included in the article's Creative Commons licence and your intended use is not permitted by statutory regulation or exceeds the permitted use, you will need to obtain permission directly from the copyright holder. To view a copy of this licence, visit <http://creativecommons.org/licenses/by/4.0/>. The Creative Commons Public Domain Dedication waiver (<http://creativecommons.org/publicdomain/zero/1.0/>) applies to the data made available in this article, unless otherwise stated in a credit line to the data.

microorganisms that have the ability to reach the environment and may pose uncommon harmful ecological and human health effects [6]. The scientific community is paying a great attention to this abnormal outstanding phenomenon of environmental pollution. Consequently, numerous environmental and toxicological studies were carried out universally to face this challengeable problem for the human safety and environmental protection [7].

Triclosan (TCS) is an antimicrobial compound with a broad-spectrum activity employed in various cosmetic and personal hygiene products such as toothpastes, deodorants, skin cosmetics and antibacterial soaps. Moreover, it is found in toys, textiles, plastics, and kitchen utensils [8]. It is considered as one of the most remarkably detected emerging contaminant in the environment [9]. It was reported that TCS and its degradation byproducts are highly toxic producing cytotoxic, genotoxic, and endocrine disruptor effects [8]. TCS was found to pose toxic effects in humans as well as aquatic species [10–13]. Furthermore, emergence of resistant bacterial strains was observed [14].

Owing to the higher toxicity of TCS, its use in Minnesota was banned by 2014, and it was applied in 2017. In Europe, TCS usage was limited in cosmetics [15]. Chlorophenols, which are metabolites of TCS, were listed to the priority toxic pollutants published by the United States Environmental Protection Agency (US-EPA) due to their higher toxicity and bioaccumulation [8].

A literature survey has shown that various techniques for TCS determination have been applied in different matrices including separation techniques such as HPLC and GC coupled with tandem mass spectrometric or ultraviolet detectors [16–21], some spectroscopic [22–25] and electrochemical reports have been published [26–28].

Electrochemical sensors are considered as a green method of analysis. Electrochemical sensors are characterized by their capability of inline monitoring of the analytes, cost-effective, minimal production of wastes and highly sensitive and selective. Potentiometric sensors (such as ion-selective electrode) are appealing for inline and continuous detection of emerging environmental contaminants. Solid contact ISEs offers several advantages over liquid state ISEs counterparts of being stable, rigid, simple, without inner filling solution and easy to miniaturize [29]. However, the existence of an aqueous layer between the solid-contact electrode and the polymeric ion selective membrane (ISM) leads to the occurrence of a potential drift which is considered as one of the principal drawbacks of solid-contact sensors. The formed water layer deteriorates both the stability and sensitivity of the sensor. Minimization of the negative impacts of the aqueous layer can be performed by incorporating a hydrophobic conductive interlayer at the interface of

ISM and the solid contact. Multi-walled carbon nanotubes (MW-CNTs) have been employed as a lipophilic ion-to-electron transducer layer at the interface of ion-selective membrane/solid-contact [30]. Furthermore, miniaturization and microfabrication have drawn great attention especially in the field of applying green chemistry. Microfabricated sensors are small, rapid, easy to use and environmentally friendly. Copper is not commonly used as electrode substrate, but there has been recent interest to utilize it as substrate due to its advantages such as cheapness compared to platinum and gold, applications in microfabrication process and printed circuit board design, and wide applications. It is worth mentioning that the literature contains few potentiometric sensors designed for TCS detection, such as liquid contact ISE impregnated with a molecularly imprinted polymer (MIP) for selective TCS determination, this proposed sensor has LOD equal  $1.9 \times 10^{-9}$  M, in spite of the fact that reported LOD is low, the MIP preparation methodology is laborious [31].

Nanoparticles have been attractive to most of the researchers owing to their incomparable characteristics and broad real-world applications. The choice and optimization of the components of a developed sensor are prerequisite for obtaining a sensor with an excellent performance [32]. An example of nanoparticles that have gained a great interest in different analytical techniques is carbon nanotubes (CNTs). CNTs are characterized by their unique structure with significant thermal and electrical properties [33]. CNTs nanocomposites have been deposited on the surface of SC-ISEs as they can minimize the signal drift which is one of the main drawbacks of SC-ISEs [34]. CNTs have been employed in ISEs as an ion to electron transducing coat and since they are lipophilic, the aqueous layer that tend to be formed between the electrode and the membrane was no longer present and therefore the long-term signal stability of the electrochemical sensor was strongly enhanced. CNTs are stable under atmospheric O<sub>2</sub> and CO<sub>2</sub> since they are nonreactive and do not experience any oxidation or reduction reactions. Furthermore, CNTs are not light sensitive. All the above disclose why CNTs are being superior to other polymers that have been utilized as transducers [35].

From this point, it is necessary to design an eco-friendly, accessible, sensitive, and rapid potentiometric sensor using three micro-fabricated solid contact potentiometric sensors for measuring and monitoring the emerging contaminant TCS in the environmental water samples. The sensor was developed and optimized on two steps: first, the MW-CNTs nanocomposite layer was incorporated for sensitivity and potential stability enhancement and the sensor performance was compared to a bare Cu solid state ISE. Second, we exploited the strong complexation between TCS and  $\beta$ -cyclodextrin

( $\beta$ -CD) for enhancing both the sensitivity and selectivity of the proposed sensor by incorporating  $\beta$ -CD in the PVC polymeric membrane [36, 37]. The proposed sensors have been validated in accordance with the IUPAC recommendations and then, exploited for TCS measurement in real environmental samples. The sensors' response was statistically compared with reported work to evaluate the validity and applicability of the microfabricated SC-ISEs.

## Experimental

### Materials

Triclosan (TCS), Multi-Walled-Carbon nanotubes (MW-CNT) and  $\beta$ -cyclodextrin (purchased from Sigma-Aldrich (Germany). Tetrahydrofuran (THF), 1-Nitro-2-octyloxybenzene (*o*-NPOE), tetra-dodecylammonium chloride (TDAC), and high molecular weight polyvinyl chloride (PVC) were obtained from Fluka. Deionized water. Other chemicals are mentioned in the supplementary materials.

### Instrumentation

- Ag/AgCl double junction – type external reference electrode (Thermo Scientific Orion 900,200, (MA, USA); 3.0 M KCl saturated with AgCl as an inner filling solution and 10%  $\text{KNO}_3$  as a bridge electrolyte) and Jenway digital ion analyzer (model 3330, Essex, UK) were used for potentiometric measurements.
- For pH adjustments, a Jenway pH glass electrode no. 924,005- BO3- Q11C (Essex, UK) was used.
- For temperature adjustments, a Bandelin Sonorex magnetic stirrer and heater, model Rx510S (Budapest, Hungaria) was used.

### Preparation of TCS stock standard solution

Preparation of 1 mM stock solution of TCS was carried out by dissolving 28.0 mg of TCS in 3 mL of NaOH and then the complete the volume to 100 mL using 0.1 M  $\text{Na}_2\text{CO}_3$  /  $\text{NaHCO}_3$  buffer (pH 10.0) in volumetric flask. The TCS stock solution was stored at 4 °C in the fridge.

### TCS working solutions

The working solutions ( $1.0 \times 10^{-4}$  –  $1.0 \times 10^{-10}$  M) were prepared from the TCS stock solution (1 mM) by dilution using 0.1 M  $\text{Na}_2\text{CO}_3$  /  $\text{NaHCO}_3$  buffer.

### Water samples collection

Water samples have been collected in amber glass bottles that has been pre-rinsed with ultra-pure water, the bottles were completely filled without any headspace remaining. Three water sources were selected, the first source was the tap drinking water sample collected from domestic water supply. The second source of water sample is water from drinking water plant before treatment,

that plant receives water supply from pipes 100 Km away from the Nile River, while the third source is water sample collected from drinking water plant just after water treatment and before distribution to other areas.

All samples have been refrigerated (at 4 °C) during transfer to the lab. Then, samples were vacuum filtered through 0.45  $\mu\text{m}$  membrane filter and stored at 4 °C without any preservative and analyzed within two days to prevent microbial contamination.

### Procedures

#### Microfabrication of the copper electrodes

The design of photomask was carried out using CAD software with specified sensor dimensions then printed using a laser printer on a transparent sheet. Pre-sensitized photoresist coated printed circuit boards (PCB) was covered with the photomask and exposure to ultraviolet light (365 nm) for 30 s was utilized to transfer the designed sensor pattern. The photomask blocks the UV irradiation on the defined dimensions, while exposes the uncovered positive photoresist. The photoresist development process was performed by agitation the PCB in NaOH solution (0.25 M) for 2 min to take off the UV irradiated photoresist. Then, exposed copper was etched using wet etching process by soaking PCB in ammonium persulfate solution (1.1 M) at 40 °C. Finally, the acetone was used to strip the remaining photoresist and expose the microfabricated copper electrode. Washing of the microfabricated Cu electrodes were done thoroughly with isopropyl alcohol and double-distilled water before use. The microfabrication steps are summarized as shown in (Fig. 1).

#### CNT-nanocomposite preparation and ion selective membrane composition

First, MW-CNT nanocomposite was prepared as reported in the literature, briefly, mixing 0.15 mg of MW-CNT with 5 mg *o*-NPOE (5  $\mu\text{L}$ ) in 1 mL THF and then sonicated for 20 min.

For both sensor 1 and 2, ISM was prepared by mixing *o*-NPOE (66.60%, 399.6 mg) with PVC (33.24%, 199.44 mg) and tetradodecylammonium chloride (0.16%, 0.96 mg) in a test tube. For sensor 3, it is prepared by mixing *o*-NPOE (66.60%, 399.6 mg) with PVC (32.19%, 199.44 mg), tetradodecylammonium chloride (0.16%, 0.96 mg), and the ionophore  $\beta$ -CD (1.05%, 6.35 mg) in a test tube, the ion exchanger to ionophore ratio was chosen to be 1:2 in order to optimize the ionophore-doped sensor response as reported in our previous work [38].

The assembly of the solid-contact potentiometric sensors was performed by direct drop-casting 10  $\mu\text{L}$  of the ISM on Cu electrodes for sensor 1 and let the ISM to dry for 24 h. While for sensors 2 and 3, a layer of CNT-nano-composite was drop-casted (10  $\mu\text{L}$ ) on Cu electrodes first

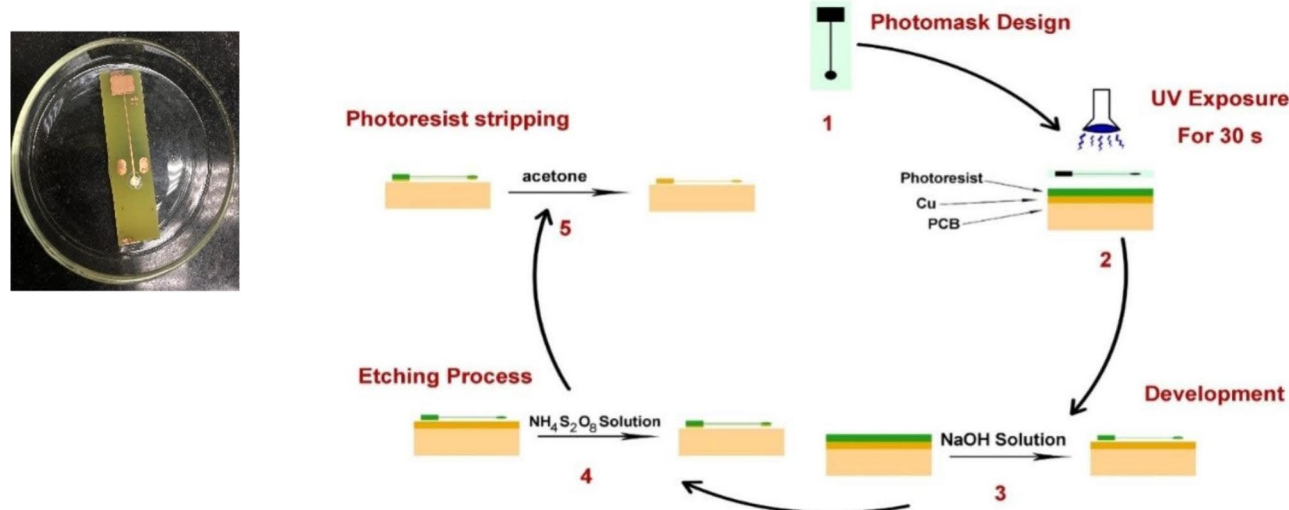


**Fig. 1** Schematic diagram of the microfabrication steps of the proposed sensors with an insert showing the real photo of the microfabricated sensor

and dried in air for 24 h, and then a 10  $\mu\text{L}$  of the corresponding ISM was drop-casted on modified Cu electrode.

#### Calibration

Calibration curves for TCS have been constructed by measuring the potential difference (electromotive force,  $\text{emf}$ ) between prepared the TCS serial dilutions against double junction reference electrode. The interfering anions calibration curves have been recorded by serial dilution of the interfering ion solution using deionized water. Selectivity coefficients have been computed using the separate solution method [39]. Limit of detection (LOD) has been calculated in accordance with the IUPAC recommendations [40].

#### Analysis of water samples using the microfabricated sensors

A volume of 5 mL of  $1 \times 10^{-6}$ ,  $1 \times 10^{-5}$ ,  $1 \times 10^{-4}$  M standard solutions have been transferred separately to 50 mL volumetric flasks then the volume was completed by the drinking tap water sample (whose pH was 10.0) to yield final concentrations  $1 \times 10^{-7}$ ,  $1 \times 10^{-6}$ , and  $1 \times 10^{-5}$  M, respectively. The three sensors were utilized to measure  $\text{emf}$  values of the prepared samples. Applying the calculated regression equations, the concentrations have been computed utilizing the obtained  $\text{emf}$  results. The concentration results are presented as recovery  $\pm$  standard deviation.

#### Investigation of the electrochemical figures of merit of fabricated sensors

According to IUPAC recommendations [41], the proposed microfabricated sensors' figures of merit such as slope, response-time, and other parameters have been evaluated.

#### Study of pH effect on sensor's performance

Studying the pH effect on the microfabricated sensors' electrochemical signal response was performed at two different concentrations ( $1 \times 10^{-4}$  and  $1 \times 10^{-5}$  M) at the pH range from 1.0 to 12.0. For each concentration, the  $\text{emf}$  was measured as a function of pH.

#### Effect of temperature

Studying the thermal effect on the designed microfabricated sensors' response was carried out. The potential response of working solutions within different concentration ranges ( $1 \times 10^{-8} - 1 \times 10^{-3}$  M) for sensor 1, ( $1 \times 10^{-9} - 1 \times 10^{-3}$  M) for sensor 2 and ( $1 \times 10^{-10} - 1 \times 10^{-3}$  M) for sensor 3 was measured at these temperature values (25, 30, 35, 40, and 45 °C). For each temperature, sensor calibration has been carried out.

#### Potentiometric aqueous layer test

The solid-state ISEs' long-term stability is highly impacted by the presence of a water layer underneath the ISM [42]. The aqueous layer formation can be assessed by measuring the potential signal drift of the sensor upon changing from the ion of interest ( $1 \times 10^{-6}$  M) to an interfering ion solution with a high concentration ( $1 \times 10^{-2}$  M of naproxen (NPR)) and then immersed into the primary ion of interest. If there was a water layer undesirable potential signal drifts will occur.

## Results and discussion

The proposed microfabricated solid-contact ISEs can determine TCS in drinking tap water samples with high sensitivity, selectivity, and lower detection limits.

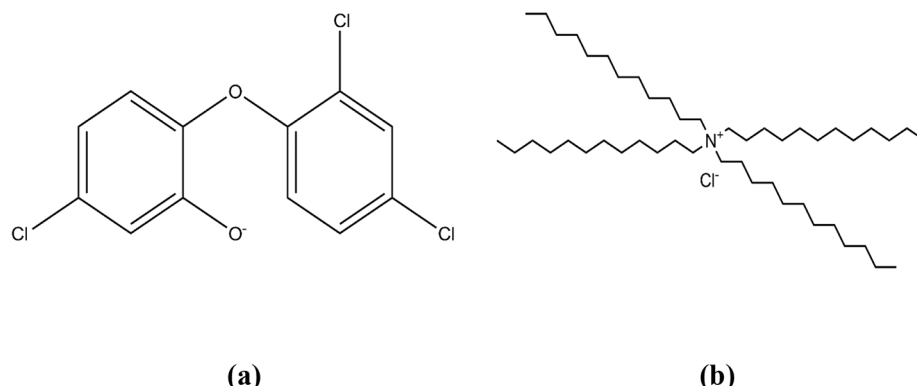


**Fig. 2** Chemical structure of (a) TCS showing its anionic site and (b) Tetra-dodecyl ammonium chloride

**Table 1** General characteristics of the three microfabricated proposed sensors

Parameter	Sensor 1	Sensor 2	Sensor 3
Slope (mV/ decade) <sup>*</sup> $\pm$ SD	$59.87 \pm 0.26$	$59.88 \pm 0.19$	$60.01 \pm 0.11$
Intercept (mV)	182.62	81.19	79.41
LOD (M) <sup>**</sup>	$9.87 \times 10^{-9}$	$9.62 \times 10^{-10}$	$9.94 \times 10^{-11}$
Response time (sec.)	12	10	10
Working pH range	7.0–11.0	7.0–11.0	7.0–11.0
Concentration linear range (M)	$1 \times 10^{-8} - 1 \times 10^{-3}$	$1 \times 10^{-9} - 1 \times 10^{-3}$	$1 \times 10^{-10} - 1 \times 10^{-3}$
Stability (days)	45	60	60
Average recovery (%) $\pm$ SD	$99.98 \pm 1.34$	$100.01 \pm 1.35$	$99.99 \pm 0.27$
Correlation coefficient	0.9999	0.9999	0.9999
Repeatability (% RSD)	1.21	0.81	0.67
Intermediate precision (% RSD)	1.51	0.97	0.95

\*Average of three determinations

\*\*Limit of detection measured by intersection of the two linear extrapolated arms of Fig. (2)

**Microfabrication of the miniaturized solid-contact sensors**  
The proposed study is based on the interaction between the anionic site present in the TCS chemical structure and the cationic exchanger tetra-dodecyl ammonium chloride as shown in Fig. 2. Their interaction was proved to be optimum and stable, by the observed Nernstian responses for the three microfabricated sensors.

The rationale behind the design of sensor 2 is that the addition of MW-CNTs might offer several advantages versus the control sensor (sensor 1). Since SC-ISEs response generally negatively influenced by the potential signal drift, plausibly due to the existence of an aqueous film beneath the membrane which may affect SC-ISEs long-term signal stability. Incorporation of hydrophobic nanomaterials that possess both electronic and ionic conductivity might act as ion-to-electron transducers between the ion selective membrane and the electronic conductor. These nanomaterials have greatly enhanced the long-term potential signal, sensitivity, and improved detection limits of the solid-state sensors [42–44]. MW-CNTs were a good candidate to act as a redox-buffering underlayer improving the long-term potential stability,

the selectivity, sensitivity, and detection limits of the proposed sensor.

Supramolecular macrocycles embedded within electrochemical sensors have been reported to enhance both sensitivity and selectivity via formation of inclusion complexes between the supramolecular host and the analyte guest [45]. For the proposed sensor 3,  $\beta$ -CD was impregnated into the ISM as an ionophore to increase the selectivity of the membrane and hence enhance the sensitivity of the electrode. The choice of  $\beta$ -CD as ionophore is based on the reported great affinity to  $\beta$ -CD towards TCS creating an inclusion complex in a 1: 1 ratio [36, 46].

#### Sensors' calibration and response time

The electrochemical characteristics of microfabricated sensors has been evaluated in accordance with the guidance of the IUPAC recommendations [47] and are represented in Table 1. Calibration curves of the proposed microfabricated sensors were plotted as shown in Fig. 3, which represents linear responses and almost ideal behavior of the monovalent anionic Nernstian slopes recorded in Table 1. The LOD was computed from the

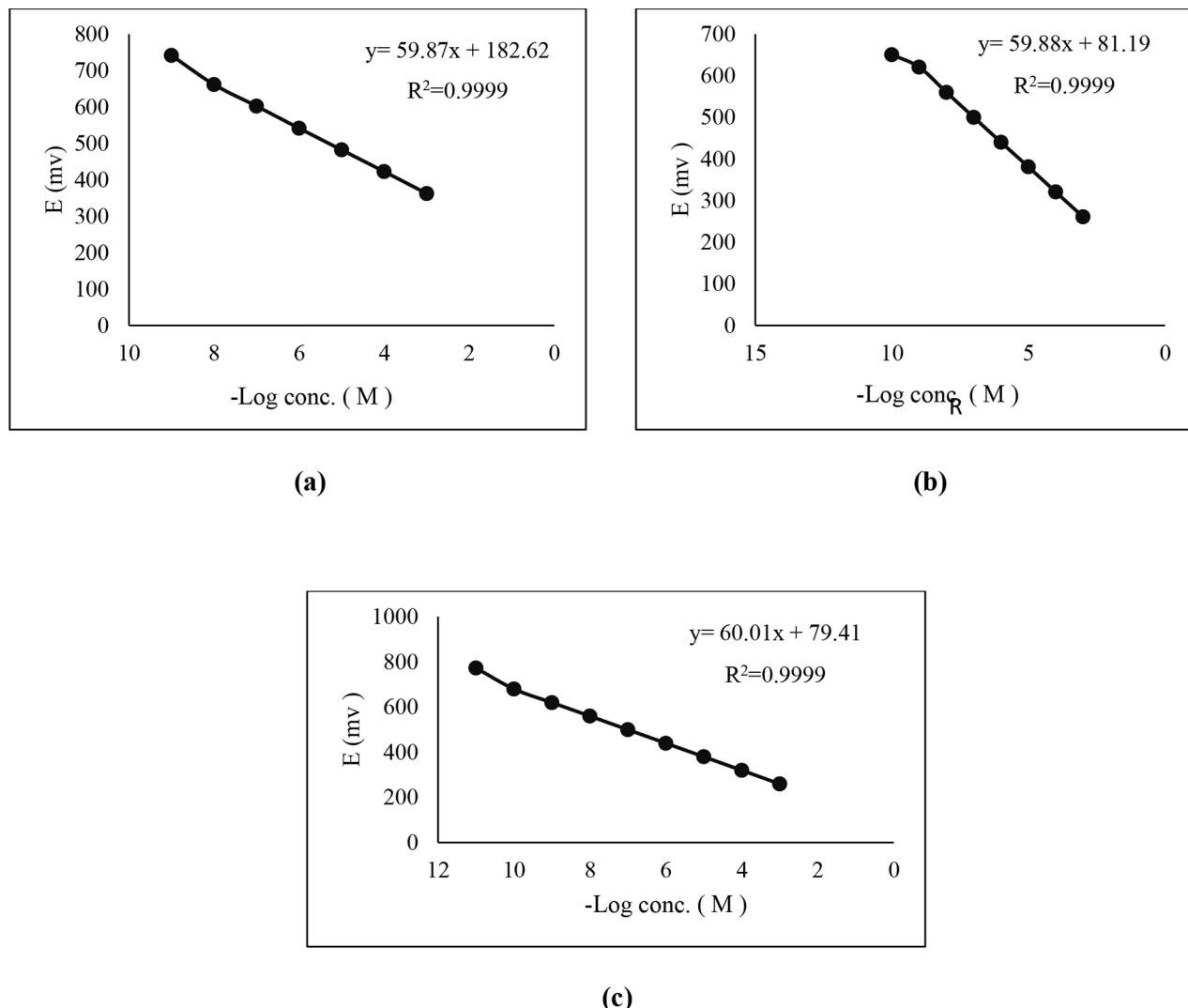


**Fig. 3** Profile of the potential in mV versus -Log concentration of TCS using the proposed microfabricated (a) sensor 1 (b) sensor 2 (c) sensor3

intersect of the two linear extrapolated parts of the calibration curve. The response time is the time required for the sensor to reach equilibrium potential value (within  $\pm 1$  mV of the final signal) after a 10-fold increment in the analyte concentration. The sensors response time was estimated.

#### Effect of pH on sensors response

The pH influence on the potential signal of the three microfabricated sensors was investigated on two concentration values ( $1 \times 10^{-4}$  and  $1 \times 10^{-5}$  M) at pH range (1.0–12.0), as shown in Fig. 4. It was concluded that pH range (7.0–11.0) is the optimal pH working range for all microfabricated sensors owing to the constant measured potential. Hydronium and hydroxyl ions may interfere at both extremes of pH values. Moreover, TCS is a phenolic derivative, once introduced into acidic pH, it becomes unionized, and hence precipitation takes place.

#### Sensors response at various temperatures

Upon studying the thermal effect on sensors response, all proposed sensors exhibited little increase of *emf* potential response by elevation of the temperature from 25 to 45 °C. It's worth noting that the obtained calibration graphs were parallel at the studied temperatures as represented in Fig. 5.

#### Effect of foreign compounds on sensor selectivity

The influence of different interfering ions upon the application of the microfabricated sensors was evaluated by SSM [41]. Results are summarized in Table 2, these results show that the sensors selectivity coefficients in the presence of some inorganic anions ( $\text{Cl}^-$ ,  $\text{NO}_3^-$ ,  $\text{Br}^-$ ,  $\text{SO}_4^{2-}$ ,  $\text{C}_2\text{O}_4^{2-}$ ,  $\text{C}_2\text{H}_3\text{CO}_2^-$ ,  $\text{PO}_4^{3-}$ ) and an emergent pollutant that might coexist (i.e., Ketoprofen). The obtained results clearly indicate that the fabricated sensors exhibit high sensitivity towards the target contaminant.

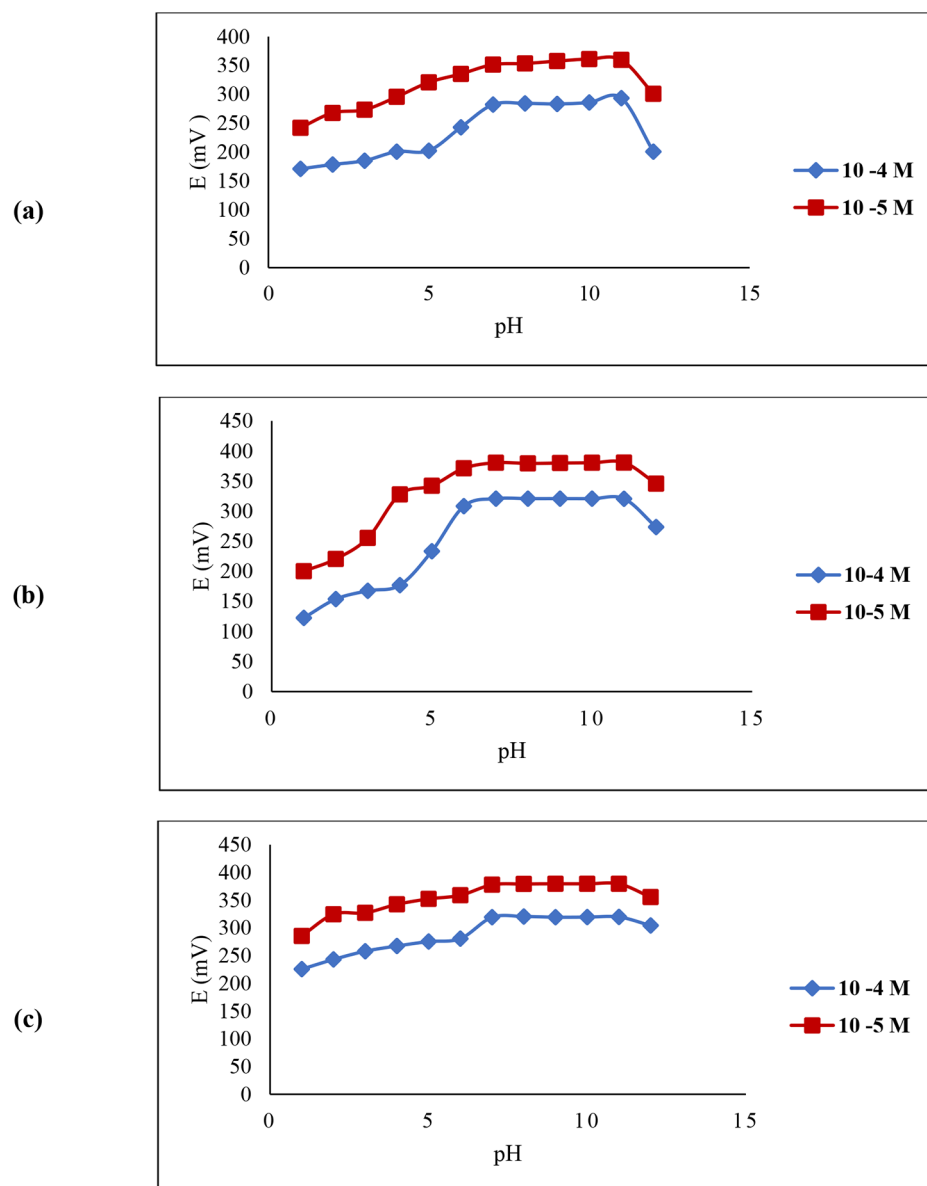


**Fig. 4** Effect of pH on the response of the proposed microfabricated (a) sensor 1 (b) sensor 2 (c) sensor3 for TCS

Moreover, sensor 3 possesses the highest selectivity in comparison to sensors (1 and 2), which can be attributed to the inclusion of  $\beta$ -CD as an ionophore.

#### Potentiometric aqueous layer test

There were not any noticeable potential drifts in the proposed sensors 2 and 3 potential response indicating that the incorporation of MW-CNT nanocomposite excluded the aqueous layers. However, due to the absence of MW-CNTs in the proposed sensor 1, an aqueous layer was formed leading to a highly significant potential drift affecting the long-term signal stability of the fabricated sensor as shown in (Fig. 6).

#### Application to the spiked water samples

The proposed sensors can be employed to determine the target contaminant in water samples with acceptable recovery percentages with minimal interferences as shown in Table 3.

As sensor 3 is highly selective, sensitive, and accurate, it has been used for TCS determination in Nile River water samples and the treated water from the water treatment plant. TCS was found in Nile River water and treated water at concentrations  $3.38 \times 10^{-6}$  M and  $1.36 \times 10^{-8}$  M, respectively.

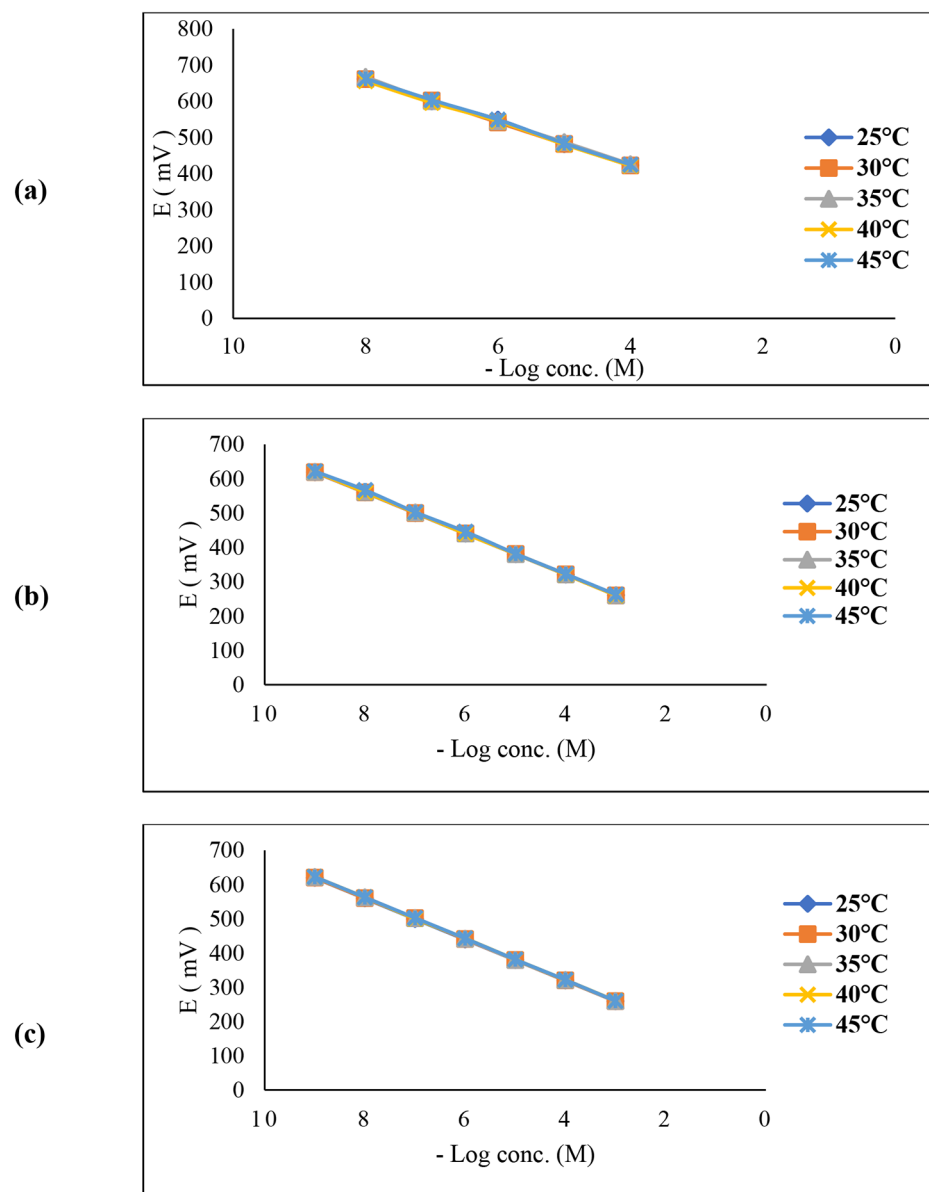


**Fig. 5** Effect of temperature on the response of the proposed microfabricated (a) sensor 1 (b) sensor 2 (c) sensor3 for TCS

**Table 2** Potentiometric selectivity coefficients ( $\log K_{\text{primary ion, Interferent}}^{\text{pot}}$ ) for the three microfabricated proposed sensors

Interferent*	Selectivity coefficient ( $\log K_{\text{primary ion, Interferent}}^{\text{pot}}$ ) for sensor 1	Selectivity coefficient ( $\log K_{\text{primary ion, Interferent}}^{\text{pot}}$ ) for sensor 2	Selectivity coefficient ( $\log K_{\text{primary ion, Interferent}}^{\text{pot}}$ ) for sensor 3
$\text{Cl}^-$	-3.334	-4.387	-4.511
$\text{NO}_3^-$	-4.139	-3.804	-4.359
$\text{Br}^-$	-3.789	-4.913	-4.518
$\text{SO}_4^{2-}$	-5.393	-5.711	-4.722
$\text{C}_2\text{O}_4^{2-}$	-5.328	-6.412	-4.451
$\text{C}_2\text{H}_3\text{CO}_2^-$	-4.631	-3.480	-4.314
$\text{PO}_4^{3-}$	-7.108	-6.135	-4.499
Ketoprofen	-4.385	-3.449	-3.763

\* Aqueous solutions of  $1 \times 10^{-4} \text{ M}$  were used

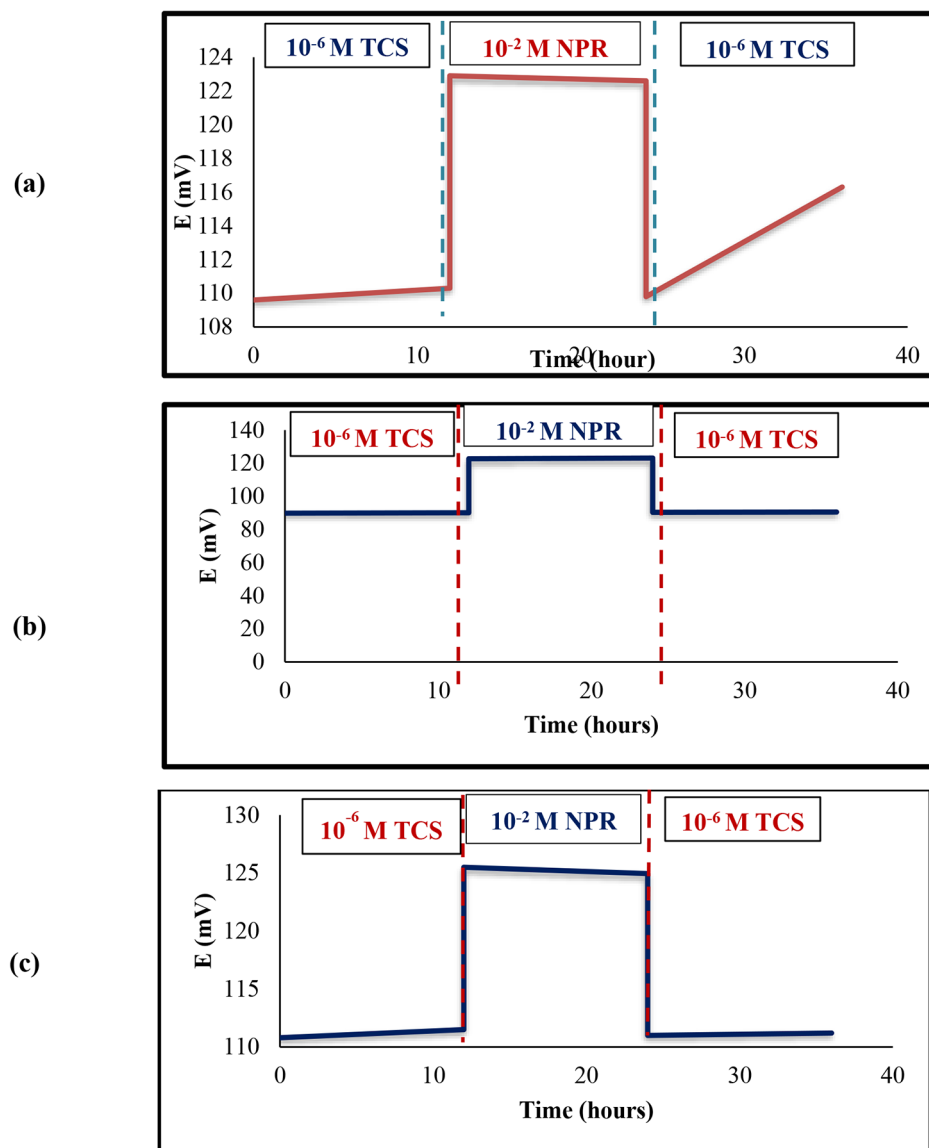


**Fig. 6** Aqueous layer test of the proposed microfabricated (a) sensor 1 (b) sensor 2 (c) sensor 3

**Table 3** Application of the three microfabricated proposed sensors on drinking water samples

TCS added conc. (M)	Sensor 1		Sensor 2		Sensor 3	
	TCS found conc. (M)	Recovery <sup>*</sup> %	TCS found conc. (M)	Recovery <sup>*</sup> %	TCS found conc. (M)	Recovery <sup>*</sup> %
$1 \times 10^{-8}$	$1.00 \times 10^{-8}$	100.00	$1.00 \times 10^{-8}$	100.00	$9.82 \times 10^{-9}$	98.20
$1 \times 10^{-6}$	$1.01 \times 10^{-6}$	101.00	$9.91 \times 10^{-7}$	99.10	$1.00 \times 10^{-6}$	100.00
$1 \times 10^{-5}$	$1.01 \times 10^{-5}$	101.00	$1.00 \times 10^{-5}$	100.00	$9.94 \times 10^{-6}$	99.40
Mean $\pm$ SD	$100.67 \pm 0.58$		$99.70 \pm 0.52$		$99.20 \pm 0.92$	

\* Average of three determinations

**Table 4** Statistical analysis of the results obtained by the proposed microfabricated sensors and the official method for the analysis of TCS

Statistical term	Official method **	Proposed sensor 1	Proposed sensor 2	Proposed sensor 3
Mean	100.24	99.98	100.01	99.99
SD	0.483	1.348	1.353	0.274
Variance	0.23	1.28	1.08	0.04
n	5	5	5	5
t		1.12 (2.31) <sup>*</sup>	1.62 (2.31) <sup>*</sup>	1.14 (2.31) <sup>*</sup>
F		5.49 (6.39) <sup>*</sup>	4.64 (6.39) <sup>*</sup>	5.35 (6.39) <sup>*</sup>

\*The theoretical values of t and F at  $P=0.05$

\*\*High performance liquid chromatography determination of TCS [48] by using a C18, 5  $\mu$  (250×4.6 mm) column, a mobile phase of methanol: water (90: 10, v/v) at flow rate 1 mL min $^{-1}$  and UV detection at  $\lambda=280$  nm using 20  $\mu$ L as an injection volume

## Statistical analysis

The results of the three proposed microfabricated sensors and the reported method were statistically compared [48]. It was performed at 95% confidence level using the student's t-test and F test as represented in Table 4. The results indicate that the difference was statistically insignificant between the fabricated and the reported method indicating good accuracy and precision.

## Greenness assessment

Electroanalysis is a promising technique of green analysis since it is a direct method where no sample collection and pretreatment steps are needed. Miniaturization of the developed sensors is eco-friendly offering the advantage of real-time measurements, the use of small sample volume and reduction of the amount of waste. The microfabrication has eliminated the use of an inner filling solution and offering the advantage of being green, simple, low cost and sensitive. Environmental monitoring is in deep need for green analytical methods development instead of the conventional hazardous methods [29, 49]. Evaluation of proposed methods using specialized greenness assessment tools is highly recommended. The National Environmental Methods Index (NEMI) is oldest greenness assessment tool [50]. Later, Analytical Eco-scale was developed. The latter was based on computing a method score by assigning penalty points to various factors in the analytical procedure to be subtracted from a 100 base [51]. Recently Green analytical procedure Index (GAPI) was developed for the greenness assessment [52]. Analytical eco-scale and GAPI tools were adopted for the greenness assessment of the proposed method.

**Table 5** The penalty points for the proposed potentiometric method using the Analytical Eco-scale method of assessment

Hazard	Penalty points for the proposed potentiometric sensors
<b>• Reagents:</b>	
$\text{Na}_2\text{CO}_3 / \text{NaHCO}_3$ buffer, pH 10	2
Water	0
<b>• Instruments:</b>	
Energy and occupational hazard	0
Waste	3
Total penalty points	5
Analytical eco-scale for the proposed methods	<b>95</b>

## Analytical eco-scale

Various factors included in the developed method were given penalty points to be subtracted from a 100 base. Excellent green analysis will be higher than 75 score, acceptable green analysis is higher than 50 and inadequate green analysis is less than 50. Penalty points are calculated based on both the type and amount of the reagent, the energy requirement of various electrical instruments, the treatment of the analytical waste and the occupational hazard [53]. The developed method eco-scale values were computed and were found to be 95 (Detailed information are provided in Table 5) and based on this assessment the proposed sensors have proved to be an excellent green analytical platform.

## Green analytical procedure index

GAPI is a recent developed greenness assessment method, that evaluates the greenness of entire procedure from the sample collection step till the final detection. It includes five pentagrams that represent each stage of the process. There are three color scale levels: green, yellow, or red indicating high, medium, and low environmental impact [52]. Figure 4 shows that the proposed sensors do not require sample preparation step, and capable of direct analysis resulting in removal of the sample preparation pentagram. Only two red regions were observed. On-line or in-line sample collection were not applicable. Therefore, to achieve a green method, no preservatives were used, and the samples were analyzed after collection within 24 h. There were no facilities to carry out waste treatment and this was the reason of the presence of another red region, but fortunately small amounts of waste were produced Fig. 7.

## Conclusion

Antimicrobial resistance that has been growing especially during the COVID-19 outbreak due to the excessive use of hand sanitizers and soaps. It is considered as a serious issue that the world must pay a great attention to control such devastating phenomenon. Regular monitoring

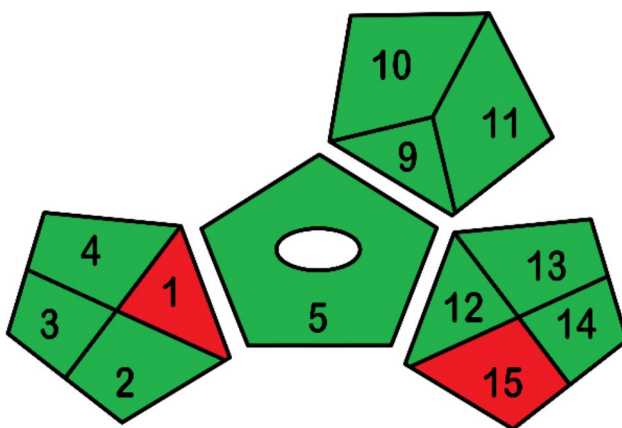


**Fig. 7** Green analytical procedure index (GAPI) tool for the proposed potentiometric sensors

of the environmental emergence of antimicrobials and the use of ecofriendly soaps and detergents is strongly recommended.

Electroanalysis is a promising green analytical technique owing to its advantages over other conventional analytical methods and can be employed for the regular monitoring of antimicrobials in the environment. Microfabrication of the used sensors with reduction of sample volume and the amount of waste produced leads to an eco-friendly method. It is worth mentioning that miniaturization of the proposed sensors offers an ease of measurement with maximum sensitivity, stability, and selectivity.

The proposed microfabricated copper ISEs allowed the ultra-trace analysis of TCS, and the incorporation of MW-CNT and  $\beta$ -CD proved to be successful in enhancing the sensitivity, selectivity, and stability of the proposed microfabricated sensors. Those sensors have many advantages as being cost-effective, disposable and can be embedded within lab-on a chip system during the micro-fabrication step for real-time continuous monitoring of TCS.

## Supplementary Information

The online version contains supplementary material available at <https://doi.org/10.1186/s13065-023-01092-0>.

Supplementary Material 1

## Acknowledgements

The authors thank the Faculty of Pharmacy, Cairo University for offering the supplies and instruments to carry out these experiments.

## Authors' contributions

NS: Visualization, Conceptualization, Investigation, Methodology, Validation, and Writing – original draft. AMM, MFAG, and MFA: Conceptualization, Investigation, and revising draft.

## Funding

This work was not supported by any funding agency or organization.

Open access funding provided by The Science, Technology & Innovation Funding Authority (STDF) in cooperation with The Egyptian Knowledge Bank (EKB).

## Data Availability

The datasets used and/or analysed during the current study available from the corresponding author on reasonable request.

## Declarations

### Ethics approval and consent to participate

N/A.

### Consent for publication

N/A.

### Competing interests

The authors declare no competing interests.

Received: 24 April 2023 / Accepted: 15 November 2023

Published online: 28 November 2023

## References

1. Daverey A, Dutta K. COVID-19: eco-friendly hand hygiene for human and environmental safety. *J Environ Chem Eng.* 2020;104754.
2. Mahmood A, Egan M, Pervez S, Alghamdi HA, Tabinda AB, Yasar A, et al. COVID-19 and frequent use of hand sanitizers; human health and environmental hazards by exposure pathways. *Sci Total Environ.* 2020;742:140561.
3. Usman M, Farooq M, Hanna K. Environmental side effects of the injudicious use of antimicrobials in the era of COVID-19. *Sci Total Environ.* 2020;745:141053.
4. Gibbs J, Stackelberg PE, Furlong ET, Meyer M, Zaugg SD, Lippincott RL. Persistence of pharmaceuticals and other organic compounds in chlorinated drinking water as a function of time. *Sci Total Environ.* 2007;373:240–9.
5. Westerhoff P, Yoon Y, Snyder S, Wert E. Fate of endocrine-disruptor, pharmaceutical, and personal care product chemicals during simulated drinking water treatment processes. *Environ Sci Technol.* 2005;39:6649–63.
6. Kuster M, López de Alda MJ, Hernando MD, Petrović M, Martín-Alonso J, Barceló D. Analysis and occurrence of pharmaceuticals, estrogens, progestogens and polar pesticides in sewage treatment plant effluents, river water and drinking water in the Llobregat river basin (Barcelona, Spain). *J Hydrol (Amst).* 2008;358:112–23.
7. Crofton KM, Paul KB, DeVito MJ, Hedge JM. Short-term in vivo exposure to the water contaminant triclosan: evidence for disruption of thyroxine. *Environ Toxicol Pharmacol.* 2007;24:194–7.
8. Bedoux G, Roig B, Thomas O, Dupont V, Le Bot B. Occurrence and toxicity of antimicrobial triclosan and by-products in the environment. *Environ Sci Pollut Res.* 2012;19:1044–65.
9. Kolpin DW, Furlong ET, Meyer MT, Thurman EM, Zaugg SD, Barber LB, et al. Pharmaceuticals, hormones, and other organic wastewater contaminants in U.S. streams, 1999–2000: a national reconnaissance. *Environ Sci Technol.* 2002;36:1202–11.
10. Foran CM, Bennett ER, Benson WH. Developmental evaluation of a potential non-steroidal estrogen: Triclosan. *Marine Environmental Research.* Elsevier; 2000. pp. 153–6.
11. Ishibashi H, Matsumura N, Hirano M, Matsuoka M, Shiratsuchi H, Ishibashi Y, et al. Effects of triclosan on the early life stages and reproduction of medaka *Oryzias latipes* and induction of hepatic vitellogenin. *Aquat Toxicol.* 2004;67:167–91.
12. Matsumura N, Ishibashi H, Hirano M, Nagao Y, Watanabe N, Shiratsuchi H, et al. Effects of Nonylphenol and Triclosan on production of plasma vitellogenin and testosterone in male South African clawed frogs (*Xenopus laevis*). *Biol Pharm Bull.* 2005;28:1748–51.
13. Ruszkiewicz JA, Li S, Rodriguez MB, Aschner M. Is Triclosan a neurotoxic agent? *J Toxicol Environ Health - Part B: Crit Reviews.* 2017;20:104–17.
14. Ricart M, Guasch H, Alberch M, Barceló D, Bonnneau C, Geisinger A, et al. Triclosan persistence through wastewater treatment plants and its potential: toxic effects on river biofilms. *Aquat Toxicol.* 2010;100:346–53.

15. Richardson SD, Kimura SY. Emerging environmental contaminants: challenges facing our next generation and potential engineering solutions. *Environ Technol Innov.* 2017;8:40–56.
16. Mohan S, Balakrishnan P. Triclosan in treated Wastewater from a City Waste-water Treatment Plant and its Environmental Risk Assessment. *Water Air Soil Pollut.* 2019;230:1–13.
17. Hua W, Bennett ER, Letcher RJ. Triclosan in waste and surface waters from the upper Detroit River by liquid chromatography-electrospray-tandem quadrupole mass spectrometry. *Environ Int.* 2005;31:621–30.
18. Silva ARM, Nogueira JMF. New approach on trace analysis of triclosan in personal care products, biological and environmental matrices. *Talanta.* 2008;74:1498–504.
19. Trenholm RA, Vanderford BJ, Holady JC, Rexing DJ, Snyder SA. Broad range analysis of endocrine disruptors and pharmaceuticals using gas chromatography and liquid chromatography tandem mass spectrometry. *Chemosphere.* 2006;65:1990–8.
20. Tohidif F, Cai Z. GC/MS analysis of triclosan and its degradation by-products in wastewater and sludge samples from different treatments. *Environ Sci Pollut Res.* 2015;22:11387–400.
21. Zang X, Chang Q, Hou M, Wang C, Wang Z. Graphene grafted magnetic microspheres for solid phase extraction of bisphenol A and triclosan from water samples followed by gas chromatography-mass spectrometric analysis. *Anal Methods.* 2015;7:8793–800.
22. Montaseri H, Forbes PBC. A triclosan turn-ON fluorescence sensor based on thiol-capped core/shell quantum dots. *Spectrochim Acta A Mol Biomol Spectrosc.* 2018;204:370–9.
23. Cabaleiro N, Peña-Pereira F, de la Calle I, Bendicho C, Lavilla I. Determination of triclosan by cuvetteless UV-vis micro-spectrophotometry following simultaneous ultrasound assisted emulsification-microextraction with derivatization: use of a micellar-ionic liquid as extractant. *Microchem J.* 2011;99:246–51.
24. Kaur I, Gaba S, Kaur S, Kumar R, Chawla J. Spectrophotometric determination of triclosan based on diazotization reaction: response surface optimization using box-behnken design. *Water Sci Technol.* 2018;77:2204–12.
25. Mpupa A, Mashile GP, Nomngongo. Vortex assisted-supramolecular solvent microextraction coupled with spectrophotometric determination of triclosan in environmental water samples. *Open Chem.* 2017;15:255–62.
26. Regiart M, Magallanes JL, Barrera D, Villarroel-Rocha J, Sapag K, Raba J, et al. An ordered mesoporous carbon modified electrochemical sensor for solid-phase microextraction and determination of triclosan in environmental samples. *Sens Actuators B Chem.* 2016;232:765–72.
27. Atar N, Eren T, Yola ML, Wang S. A sensitive molecular imprinted surface plasmon resonance nanosensor for selective determination of trace triclosan in wastewater. *Sens Actuators B Chem.* 2015;216:638–44.
28. Yola ML, Atar N, Eren T, Karimi-Maleh H, Wang S. Sensitive and selective determination of aqueous triclosan based on gold nanoparticles on polyoxometalate/reduced graphene oxide nanohybrid. *RSC Adv.* 2015;5:65953–62.
29. Wang J. Real-time electrochemical monitoring: toward green analytical chemistry. *Acc Chem Res.* 2002;35:811–6.
30. El-Rahman MKA, Al-Alamein AMA, Abdel-Moety EM, Fawaz EM. Integrated Gold-Thiol based Potentiometric sensors for in situ dual drug-protein binding studies on Naproxen/Diphenhydramine salts Model. *J Electrochem Soc.* 2017;164:H1013–20.
31. Liang R, Kou L, Chen Z, Qin W. Molecularly imprinted nanoparticles based potentiometric sensor with a nanomolar detection limit. *Sens Actuators B Chem.* 2013;188:972–7.
32. Zhu C, Yang G, Li H, Du D, Lin Y. Electrochemical Sensors and biosensors based on nanomaterials and nanostructures. *Anal Chem.* 2015;87:230–49.
33. Iijima S. Helical microtubules of graphitic carbon. *Nature.* 1991;354:56–8.
34. Mahmoud AM, Abd El-Rahman MK, Elghobashy MR, Rezk MR. Carbon nanotubes versus polyaniline nanoparticles; which transducer offers more opportunities for designing a stable solid contact ion-selective electrode. *J Electroanal Chem.* 2015;755:122–6.
35. Crespo GA, Macho S, Bobacka J, Rius FX. Transduction mechanism of carbon nanotubes in solid-contact ion-selective electrodes. *Anal Chem.* 2009;81:676–81.
36. Jug M, Kosalec I, Maestrelli F, Mura P. Analysis of triclosan inclusion complexes with  $\beta$ -cyclodextrin and its water-soluble polymeric derivative. *J Pharm Biomed Anal.* 2011;54:1030–9.
37. Safwat N, Mahmoud AM, Abdelghany M, Ayad F. In situ monitoring of Triclosan in Environmental Water with Subnanomolar detection limits using eco-friendly Electrochemical sensors modified with cyclodextrins. *Environ Sci Process Impacts.* 2021. <https://doi.org/10.1039/d0em00387e>
38. Mousavi MPS, Abd El-Rahman MK, Mahmoud AM, Abdelsalam RM, Bühlmann P. In situ sensing of the Neurotransmitter Acetylcholine in a dynamic range of 1 nM to 1 mM. *ACS Sens.* 2018;3:2581–9.
39. Bakker E, Pretsch E, Bühlmann P. Selectivity of potentiometric ion sensors. *Anal Chem.* 2000;72:1127–33.
40. Lindner E, Umezawa Y. Performance evaluation Criteria for Preparation and Measurement of Macro- and Microfabricated Ion- Selective electrodes (IUPAC technical report). *Pure Appl Chem.* 2008;80:85.
41. UMEZAWA1 Y, BÜHLMANN1 P, UMEZAWA2 K, TOHDA1 K, AMEMIYA1 AS. Potentiometric selectivity coefficients of ion-selective electrodes. Part I. Inorganic cations (technical report). *Pure and Applied Chemistry.* 2009;72:1851–2082.
42. De Marco R, Veder JP, Clarke G, Nelson A, Prince K, Pretsch E, et al. Evidence of a water layer in solid-contact polymeric ion sensors. *Phys Chem Chem Phys.* 2008;10:73–6.
43. Nikolskii BP, Materova EA, SOLID CONTACT IN. MEMBRANE ION-SELECTIVE ELECTRODES. *Ion-selective Electrode Reviews.* 1985;7:3–39.
44. Bobacka J, Ivaska A, Lewenstam A. Potentiometric ion sensors. *Chem Rev.* 2008;108:329–51.
45. Luo H, Chen LX, Ge QM, Liu M, Tao Z, Zhou YH, et al. Applications of macrocyclic compounds for electrochemical sensors to improve selectivity and sensitivity. *J Incl Phenom Macrocycl Chem.* 2019;95:171–98.
46. Loftsson T, Leeves N, Björnsdóttir B, Duffy L, Masson M. Effect of cyclodextrins and polymers on triclosan availability and substantivity in toothpastes in vivo. *J Pharm Sci.* 1999;88:1254–8.
47. Umezawa Y, Bühlmann P, Umezawa K, Tohda K, Amemiya S. International Union of Pure and Applied Chemistry, Analytical Chemistry Division, Commission on Analytical Nomenclature. In: *Pure Appl. Chem. F. Kadırgan* (Turkey); 2000. p. 1851–2082.
48. Baranowska I, Magiera S, Bortniczuk K. Reverse-phase HPLC method for the simultaneous analysis of triclosan and triclocarban in surface waters. *Water Sci Technol Water Supply.* 2010;10:173–80.
49. Mohamed HM. Green, environment-friendly, analytical tools give insights in pharmaceuticals and cosmetics analysis. *TrAC - Trends in Analytical Chemistry.* 2015;66:176–92.
50. Keith LH, Gron LU, Young JL. Green Anal Methodologies Chem Rev. 2007;107:2695–708.
51. Tobiszewski M, Marć M, Galuszka A, Namieśnik J. Green chemistry metrics with special reference to green analytical chemistry. *Molecules.* 2015;20:10928–46.
52. Plotka-Wasyłka J. A new tool for the evaluation of the analytical procedure: Green Analytical Procedure Index. *Talanta.* 2018;181:204–9. September 2017.
53. Galuszka A, Migaszewski ZM, Konieczka P, Namieśnik J. Analytical Eco-scale for assessing the greenness of analytical procedures. *TrAC - Trends in Analytical Chemistry.* 2012;37:61–72.

## Publisher's Note

Springer Nature remains neutral with regard to jurisdictional claims in published maps and institutional affiliations.